

BÉZIER DESCRIPTION OF SPACE TRAJECTORIES

Francesco de Dilectis*, Daniele Mortari[†], and Renato Zanetti

Bézier curves are highly versatile polynomial curves that can be used to estimate a spacecraft trajectory based solely on measurements acquired, eventually, with on-board sensors. These measurements, weighed accordingly to their accuracy, determine the control points of the curve via a least square best fitting approach. This approach has the advantage of being independent from the problem's physics, thus giving it great generality. It is also computationally efficient, making it a valid candidate for on-board use, thus giving a spacecraft autonomy in regard to estimate its own position. Several types of trajectories are simulated for the case of Keplerian orbits and a cislunar trajectory, and artificial noise is superimposed to the measurements. The performance of the method is compared with a Weighed Iterative Least Square and an Extended Kalman Filter.

INTRODUCTION

Exact orbit determination is completely solvable only for the Two Body Problem and a few restricted cases involving three bodies. The search for solutions in more general cases has led to many important advancements in mathematics in the last 400 years[2]. Many approaches have been used, formulating the issue as an Initial Value Problem, or a Two Points Boundary Value Problem [3][4]. In other cases, especially since orbit determination has become necessary for satellites and not just for planets, statistical or filter-based techniques have been developed [5][6]. In general however, most of the times the solution is specifically tailored for the application [7][8][9].

In this paper we propose an estimation method, the theory of which has been developed very recently[1], that works independently from the physics involved, and uses only position measurements and the mathematical model of a Bézier curve in 3-D space. Such curve is defined as a polynomial function of a parameter s and a set of “control points”, organized in a $3 \times n$ matrix \mathbb{C} , where n is the curve degree. While \mathbb{C} is the ultimate target of the estimation, as any Bézier curve is completely described by its control points, as an intermediate step the values of the parameter s corresponding to the chosen measurements have to be found. This leads to an iterative process involving two different but connected least square problems, one to find the control points and the other to find the parameter values, either being function of the other. The solution is considered achieved once a certain measure of the error, defined as the difference between estimates and measurements, is under a chosen tolerance. Then, a second Bézier curve is used to approximate the behaviour of time along the trajectory. Computation of this second curve is not subject to an iterative process, because it uses the set of parameter values found for the “space” curve. Further details

*PhD Graduate Student, 301B Reed McDonald, Aerospace Engineering, Texas A&M University, College Station, TX 77843-3141. E-mail: F.DE.DILECTIS@NEO.TAMU.EDU

[†]Professor, 746C H.R. Bright Bldg., Aerospace Engineering, Texas A&M University, College Station, TX 77843-3141, AAS Fellow, AIAA Associate Fellow. IEEE Senior member. E-mail: MORTARI@TAMU.EDU

are given in the following sections. This method is used to estimate both segments of Keplerian trajectories and of a cislunar trajectory.

BÉZIER LEAST SQUARE

In this section we summarize the results of [1]. A Bézier curve of degree n is of the form:

$$\mathbf{r} = \sum_{k=0}^n \mathbf{c}_k B_k^n(s) \quad \text{where} \quad B_k^n(s) = \binom{n}{k} s^k (1-s)^{n-k}, \quad s \in [0, 1]. \quad (1)$$

By choosing a set $\{\mathbf{r}_1, \dots, \mathbf{r}_m\}$ of positions along the curve, they can be rewritten in a linear system:

$$\underset{3 \times m}{\mathbb{R}} = \underset{3 \times (n+1)}{\mathbb{C}} \underset{(n+1) \times (n+1)}{\mathbb{M}} \underset{(n+1) \times m}{\mathbb{S}} \quad (2)$$

where

$$\begin{cases} \mathbb{R} = [\mathbf{r}_1, \mathbf{r}_2, \dots, \mathbf{r}_m] \\ \mathbb{C} = [\mathbf{c}_0, \mathbf{c}_1, \dots, \mathbf{c}_n] \end{cases} \quad \text{and} \quad \mathbb{S} = \begin{bmatrix} s_1^n & s_2^n & \dots & s_{m-1}^n & s_m^n \\ \vdots & \vdots & \ddots & \vdots & \vdots \\ 1 & 1 & \dots & 1 & 1 \end{bmatrix} \quad (3)$$

and the elements of matrix \mathbb{M} are of the form $\mathbb{M}(k, j) = \binom{n}{k} \binom{n-k}{j} (-1)^{n-(k+j)}$, $j = 1, \dots, n-1$.

Eq. (2) can readily be solved for \mathbb{C} with a Least Square approach, leading to:

$$\mathbb{C} = \mathbb{R} \mathbb{S}^T (\mathbb{S} \mathbb{S}^T)^{-1} \mathbb{M}^{-1}. \quad (4)$$

Distribution of the parameter

To solve Eq. (4), a distribution of the parameter s corresponding to the measurements has to be assumed. If the data is provided at constant time step, uniform distribution can be used:

$$s_k = \frac{k-1}{n-1} \quad \text{where} \quad k \in [1, n]. \quad (5)$$

Another valid approximation relates the distribution with the relative distance of subsequent data points, as per the following:

$$\begin{cases} s_1 = 0 \\ s_m = 1 \end{cases} \quad \text{and} \quad s_k = \frac{\sum_{j=2}^k |\tilde{\mathbf{r}}_j - \tilde{\mathbf{r}}_{j-1}|}{\sum_{j=2}^m |\tilde{\mathbf{r}}_j - \tilde{\mathbf{r}}_{j-1}|} \quad \text{where} \quad k \in [2, m-1]. \quad (6)$$

In general, however, solving Eq. (4) with either distribution will lead to estimates displaced from the actual measurements, by a value of:

$$d_k = |\mathbb{C} \mathbb{M} \mathbf{s}_k - \tilde{\mathbf{r}}_k| \quad k \in [1, m]. \quad (7)$$

where \mathbf{s}_k is a vector of all the powers of s_k . Obviously, changing a certain s_k will only affect the value of the corresponding d_k . Thus, it is possible to find a new set of parameters by minimizing an aptly chosen cost function L_k , independently for each k :

$$L_k = (\mathbb{C} \mathbb{M} \mathbf{s}_k - \tilde{\mathbf{r}}_k)^T (\mathbb{C} \mathbb{M} \mathbf{s}_k - \tilde{\mathbf{r}}_k) \quad (8)$$

Applying the necessary condition for a stationary point leads to a polynomial in s_k :

$$F(s_k) = \mathbf{s}_k^T \mathbf{M} \mathbf{C}^T \mathbf{C} \mathbf{M} \frac{d\mathbf{s}_k}{ds_k} - \tilde{\mathbf{r}}_k^T \mathbf{C} \mathbf{M} \frac{d\mathbf{s}_k}{ds_k} = 0 \quad (9)$$

which can be solved numerically, for instance via Newton-Raphson method, given an initial guess \bar{s}_k , which in our application can be the value of s_k from the previous iteration. Indeed:

$$s_k^* = \bar{s}_k - \frac{F(\bar{s}_k)}{F'(\bar{s}_k)} \quad (10)$$

Minimizing Eq. (8) independently for each $k \in [2, m-1]$ (the first and last point are left unchanged, to ensure the parameter always spans the range $[0, 1]$) leads to a new parameter distribution, that can in turn be used in Eq. (4) to find a new set of control points. This process can be iterated multiple times until a certain convergence criteria has been met. The Frobenius norm of the error matrix, defined as the difference between the estimated and the measured positions, has been used in this paper analysis:

$$\left| \hat{\mathbf{R}} - \tilde{\mathbf{R}} \right|_F < \varepsilon \quad (11)$$

Degree of the Bézier curve

As is to be expected with polynomial functions, Bézier curves of different degree provide different levels of approximation. Since all but the simplest trajectories have variable curvature, and small values of curvature are often masked by noise (Fig. (1)), it is not possible to define *a priori* the optimal degree to use in a specific application. In general however, for trajectories which are more curve, in a intuitive sense, polynomials of higher degree will have better performances. On the other hand, the maximum degree usable for a given segment is limited by the number of data points available, namely:

$$n = \left\lceil \frac{m}{3} - 1 \right\rceil. \quad (12)$$

Moreover, as n increases the matrix \mathbb{S} becomes progressively ill-conditioned, because the first columns, being n -th powers of numbers less than 1 become smaller and smaller, while the last column is always made of 1. In turn, the matrix $\mathbb{S}\mathbb{S}^T$ also becomes ill-conditioned and numerical issues arise. Therefore, the algorithm finds Bézier curves at increasing degree, starting at $n = 2$, until the average position error along the curve has reached a minimum, or the degree is equal to the “hard” limit enforced by Eq. (12) or the “soft” limit enforced by the numerical problems discussed above. Other stopping criteria can be implemented, with slightly different resulting performances. In most cases, the optimal degree found iteratively will be close or equal to the maximum defined by Eq. (12).

Non-linear Time Best Fitting

In the same way as it has been done for position, also time along the trajectory can be expressed as a function of the parameter s . When measurements are taken at constant timestep, the implicit assumption is that t varies linearly with the parameter, as in $t = t_i(1-s) + t_f s$, which can be seen as a Bézier curve of degree 1. However, non-linear time models better accommodate velocity variations along the trajectory. Therefore, higher degree curves can be used to describe time, and not necessarily of the same degree used for the trajectory. In principle, the two curves exist in different dimensional spaces, with the “time curve” being effectively one dimensional. However, they still are

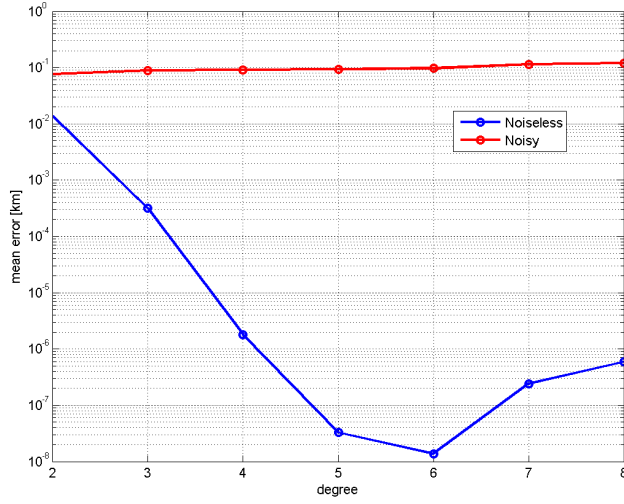


Figure 1. Optimal degree with and without noise for slightly curved trajectory. When noise is present the difference in accuracy is almost non-existent.

related via the parameter s , because each measurement is associated with a time instant. Therefore, upon reaching convergence in the estimation of the s_k , the control points τ for the “time curve” are easily found by applying the same procedure as above:

$$\tilde{\mathbf{t}} = \tau \mathbf{M}_p \mathbf{S}_p \rightarrow \tau = \tilde{\mathbf{t}} \mathbf{S}_p^T (\mathbf{S}_p \mathbf{S}_p^T)^{-1} \mathbf{M}_p^{-1} \quad (13)$$

where the subscript “ p ” is used to highlight that the polynomial degree used in this calculation is not the same used for the estimation of the position.

To summarize, the overall algorithm is described in the following flowchart:

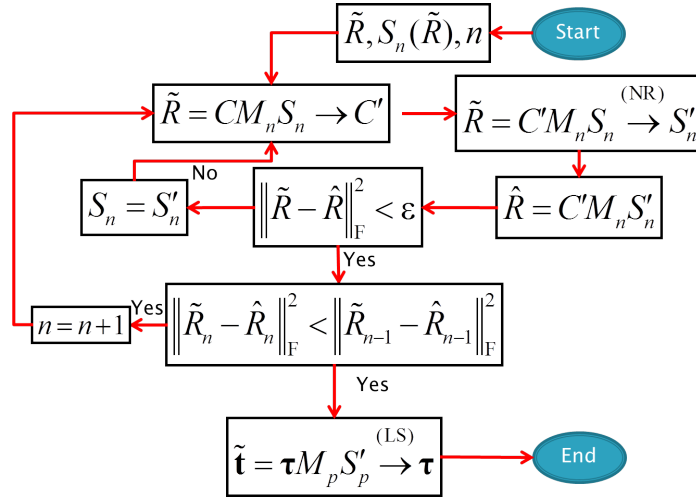


Figure 2. Algorithm scheme

Estimate of the velocity

As an added result of the method, once the “space” and “time” curve have been found, it is straightforward to obtain an estimate for the velocity at the measured positions; indeed:

$$\mathbf{v}(t) = \frac{d\mathbf{r}}{dt} = \left(\frac{d\mathbf{r}}{ds} \right) \left(\frac{ds}{dt} \right) = \left(\frac{d\mathbf{r}}{ds} \right) \left(\frac{dt}{ds} \right)^{-1} \quad (14)$$

Because both $\mathbf{r}(s)$ and $t(s)$ are simple polynomials, these derivatives are extremely simple to find. It is worth noting that Eq. (14) does not return the Bézier curve for the velocity (i.e. its control points), but only the estimated velocity at the s_k .

WEIGHTS OF THE MEASUREMENTS

The next logical step is extending the method by including relative weights for the measurements. This can be easily done, from a mathematical point of view, simply by comparing Eq. (2) with the classic equations for Weighed Least Squares. Considering a diagonal matrix of weights \mathbb{W} :

$$\min_{\mathbb{C}} (\mathbb{C}\mathbb{M}\mathbb{S} - \mathbb{R})^T \mathbb{W} (\mathbb{C}\mathbb{M}\mathbb{S} - \mathbb{R}) = \min_{\mathbb{C}} \mathbb{S}^T \mathbb{M} \mathbb{C}^T \mathbb{W} \mathbb{C} \mathbb{M} \mathbb{S} - 2\mathbb{R}^T \mathbb{W} \mathbb{C} \mathbb{M} \mathbb{S} + \mathbb{R}^T \mathbb{W} \mathbb{R} \quad (15)$$

$$\frac{d\mathbb{K}}{d\mathbb{C}} = \mathbb{C}(\mathbb{M}\mathbb{S}\mathbb{W}\mathbb{S}^T\mathbb{M}) - \mathbb{R}\mathbb{W}\mathbb{S}^T\mathbb{M} = 0 \quad (16)$$

$$\mathbb{C}(\mathbb{M}\mathbb{S}\mathbb{W}\mathbb{S}^T\mathbb{M}) = \mathbb{R}\mathbb{W}\mathbb{S}^T\mathbb{M} \quad \rightarrow \quad \mathbb{C} = \mathbb{R}\mathbb{W}\mathbb{S}^T\mathbb{M}(\mathbb{M}\mathbb{S}\mathbb{W}\mathbb{S}^T\mathbb{M})^{-1} \quad (17)$$

which results into the following expression:

$$\mathbb{C} = \mathbb{R}\mathbb{W}\mathbb{S}^T(\mathbb{S}\mathbb{W}\mathbb{S}^T)^{-1}\mathbb{M}^{-1} \quad (18)$$

Conversely, the problem of choosing the weights is not at all easy. Because they are dependent on the sensors and/or the methods used to obtain the measurements, each set is specific to the mission and generalizations cannot be made. Furthermore, in several cases the only way to obtain a reasonable approximation is via Monte Carlo simulations.

For instance, when generating measurements from analysis of images of celestial bodies, as it is assumed in the cislunar trajectory simulation in this paper, the precision of such measurements is dependent primarily on the relative distance between observer and target, if the sensor properties can be assumed constant throughout the mission, according to the following relationship:

$$\frac{dr}{dD} = -\frac{f R D}{(D^2 - R^2)^{3/2}} \quad \rightarrow \quad \sigma_D^2 = \frac{(D^2 - R^2)^3}{f^2 R^2 D^2} \sigma_r^2 \quad (19)$$

ESTIMATION OF KEPLERIAN CLOSED ORBITS

In the following section the Bézier method is used to estimate several closed Keplerian orbits, by simulating a series of measurements with artificial Gaussian noise superimposed ($\sigma_r = 1$ Km). Because these are all similar planar curves, their orientation in space is irrelevant and therefore the only orbital parameter which will affect the performance of the method is the eccentricity. . As Non-Rational Bézier curves are not suited to describe closed curves, the analysis is limited to fractions of a period, rather than the whole duration.

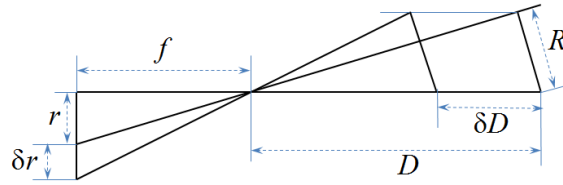


Figure 3. Distance estimation sensitivity geometry

We consider three different values of eccentricity (0.05, 0.5, 0.7), as representative for almost circular orbits, medium eccentric orbits and highly eccentric orbits. All the orbits have a perigee of 300 Km above the surface of Earth. A “sliding window” of fixed duration, but always consisting of 30 measurements, is considered moving along the orbit, until a full period is completed. In this way, it is possible to obtain the average and standard deviation for each segment as a function of the initial point of the trajectory. The plots also show which degree was found as optimal in every case. By using Eq. (14), an estimate of the velocity is also plotted.

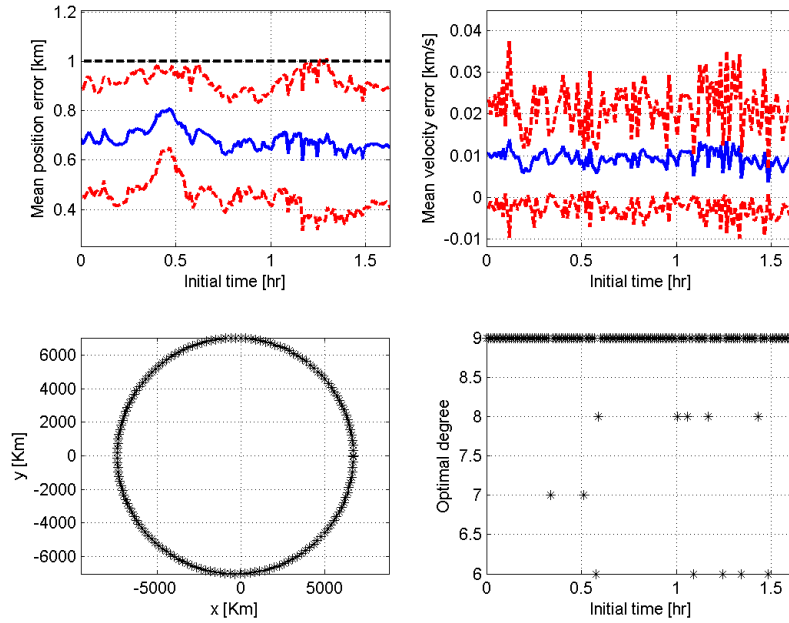


Figure 4. Segment duration: 20% T (19.55 min). Eccentricity = 0.05.

ESTIMATION OF A CISLUNAR TRAJECTORY

As a second test, Bézier Least Squares is used to estimate segments of a cislunar trajectory for a Earth-to-Moon mission. The measurements are obtained with a camera of focal length 300mm and random noise, whose standard deviation is based on the optical properties of the sensor, is artificially added. Using Eq. (19), it is possible to introduce weights in the formulation, as the the reciprocal of σ_D^2 . Along the trajectory, three segments are considered, close to the Earth, midway, and close to the Moon. Each segment consists of 25 measurements.

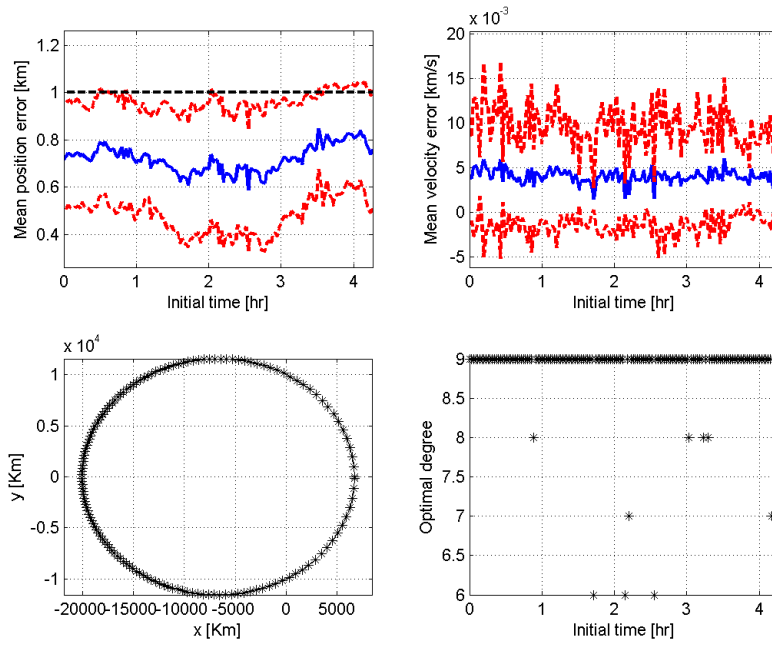


Figure 5. Segment duration: 20% T (51.20 min). Eccentricity = 0.5.

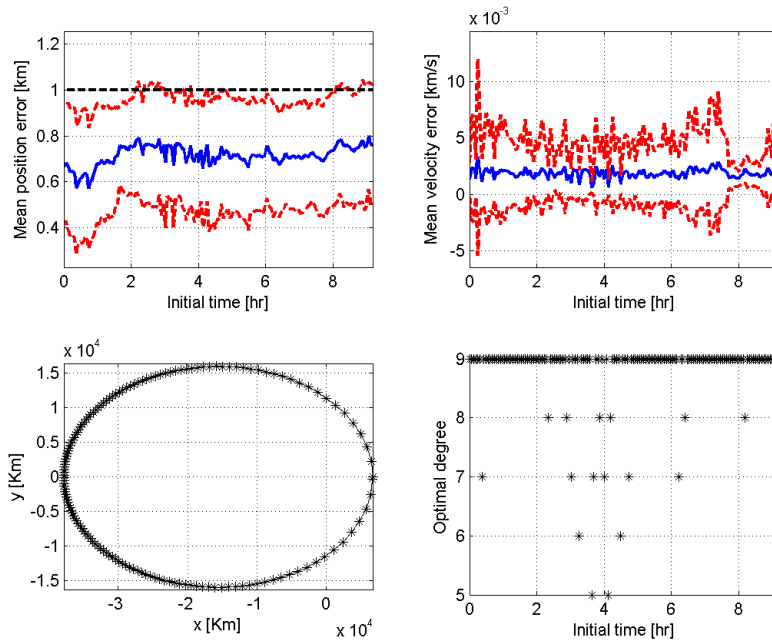


Figure 6. Segment duration: 20% T (110.2 min). Eccentricity = 0.7.

The results show the performance of our method point by point along the segments, compared with a Weighed Iterative Least Square and an Extended Kalman Filter, both of which, it's worth

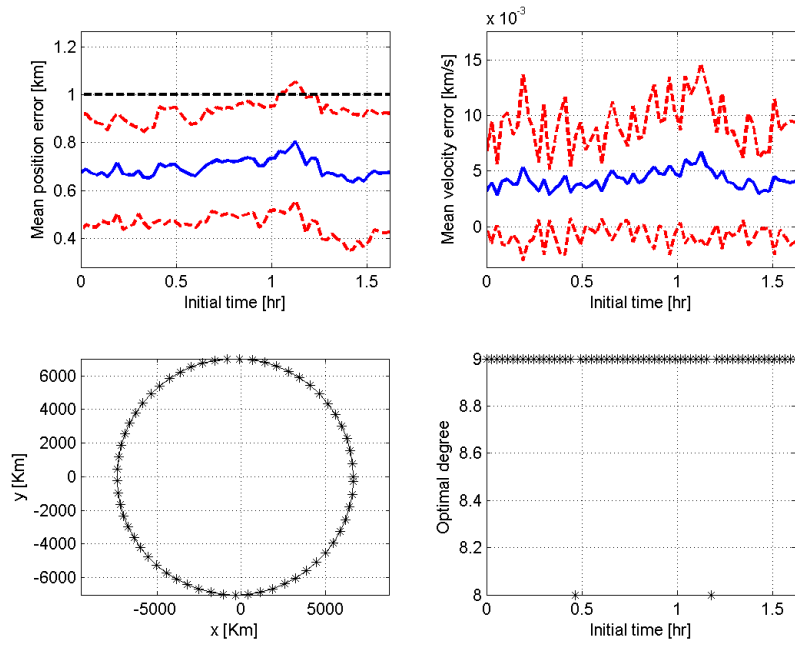


Figure 7. Segment duration: $50\%T$ (48.9 min). Eccentricity = 0.05.

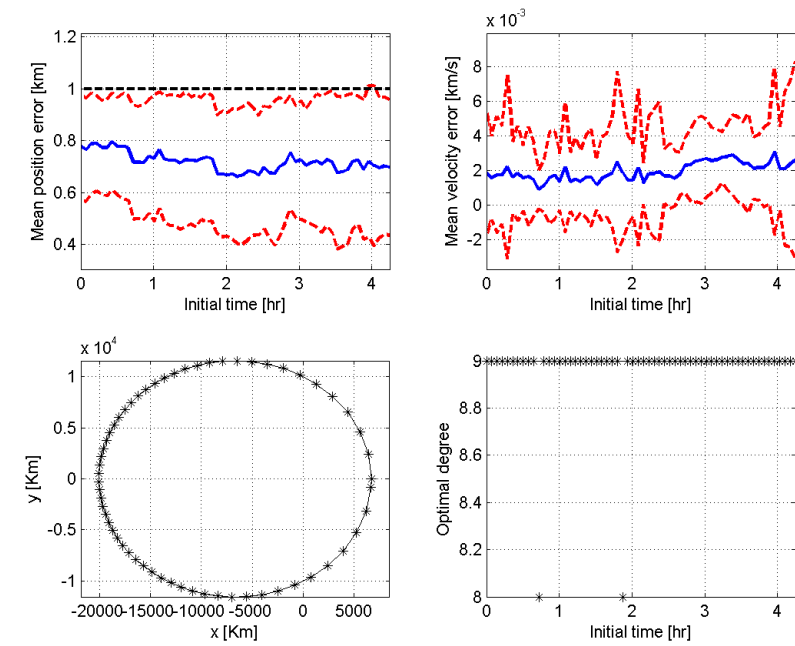


Figure 8. Segment duration: $50\%T$ (128 min). Eccentricity = 0.5.

reminding, require the propagation of a state to compute their estimate.

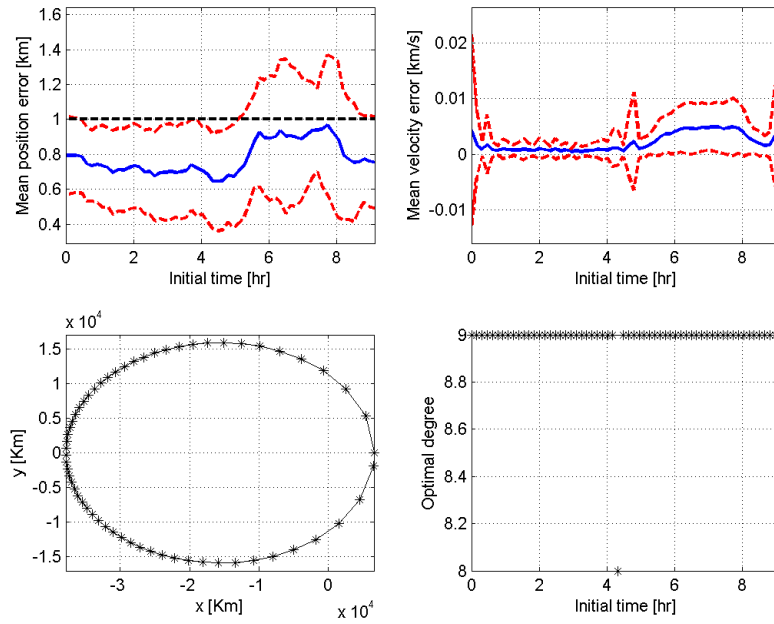


Figure 9. Segment duration: $50\%T$ (275 min). Eccentricity = 0.7.g

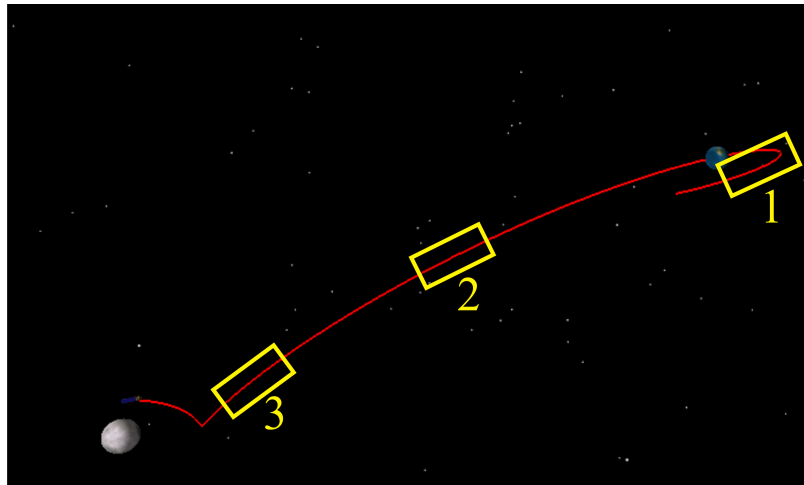


Figure 10. Simulated Earth-to-Moon trajectory (GMAT)

Weighed Iterative Least Square

The standard batch least-squares orbit determination technique [10] is used as a mean to assess the performance of the proposed method. Rather than processing the Moon direction \tilde{b}_k and Radius \tilde{R}_k separately, a single derived measurement is obtained. From the apparent Moon radius and the focal length, the “measured” distance from the Moon $\tilde{\rho}_k$ is deduced. Then a measurement \tilde{y}_k of the

vehicle position from the center of the Moon is calculated

$$\tilde{\mathbf{y}}_k = \tilde{\rho}_k C_k^T \tilde{\mathbf{b}}_k = f \frac{R_\zeta}{\tilde{R}_k} C_k^T \tilde{\mathbf{b}}_k \quad (20)$$

where R_ζ is the Moon radius, f is the camera focal length, and C_k is the J2000-to-camera attitude.

To obtain the batch least-squares solution we start from an initial estimate $\hat{\mathbf{x}}_0^T = \{\hat{\mathbf{r}}_0^T, \hat{\mathbf{v}}_0^T\}$ and propagate it forward to each measurement time using Earth and Moon's central gravities. Together with the state we integrate the state transition matrix $\Phi(t_k, t_0)$ that takes linearized state deviations from the time of the initial estimate to the time of the k -th measurement. At each measurement time we accumulate the current observation:

$$\tilde{H}_k = [I_{3 \times 3} \quad 0_{3 \times 3}] \quad (21)$$

$$H_k = \Phi(t_k, t_0) \quad (22)$$

$$\Lambda = \Lambda + H_k^T W_k H_k \quad (23)$$

$$N = N + H_k^T W_k [\tilde{\mathbf{y}}_k - (\mathbf{r}_{mk} - \hat{\mathbf{r}}_k)] \quad (24)$$

where Λ and N are initialized at zero, \tilde{H}_k is the partial of the measurement with respect to the current state, H_k is the partial of measurement with respect to the initial state, $\hat{\mathbf{r}}_k$ is the estimated position of the vehicle with respect to the center of Earth and \mathbf{r}_{mk} is the position of the Moon also with respect to Earth. The measurement weight W_k is given by the inverse of the measurement error covariance Σ_k .

$$W_k = \Sigma_k^{-1} \quad (25)$$

$$\begin{aligned} \Sigma_k &= \sigma_R^2 \begin{pmatrix} \frac{\partial \tilde{\mathbf{y}}_k}{\partial \tilde{R}_k} \end{pmatrix} \begin{pmatrix} \frac{\partial \tilde{\mathbf{y}}_k}{\partial \tilde{R}_k} \end{pmatrix}^T + \sigma_b^2 \begin{pmatrix} \frac{\partial \tilde{\mathbf{y}}_k}{\partial \tilde{\mathbf{b}}_k} \end{pmatrix} \begin{pmatrix} \frac{\partial \tilde{\mathbf{y}}_k}{\partial \tilde{\mathbf{b}}_k} \end{pmatrix}^T \\ &= \sigma_R^2 f^2 \frac{R_\zeta^2}{\tilde{R}_k^4} C_k^T \tilde{\mathbf{b}}_k \tilde{\mathbf{b}}_k^T C_k + \sigma_b^2 \tilde{\rho}_k^2 (\mathbf{I} - C_k^T \tilde{\mathbf{b}}_k \tilde{\mathbf{b}}_k^T C_k) \end{aligned} \quad (26)$$

where σ_R^2 is the variance of the error in determining the Moon radius and σ_b^2 is the variance of the error in determining the Moon direction.

After all measurements are accumulated the initial estimate is updated as:

$$\hat{\mathbf{x}}_0 = \hat{\mathbf{x}}_0 + \Lambda^{-1} N \quad (27)$$

This procedure can be iterated multiple times.

Extended Kalman Filter

The extended Kalman filter incorporates one measurement at the time rather than using all of them at once. Therefore using the EKF algorithm only the estimate at the very last measurement time contains information from all the measurements. This is in contrast with the batch least-squares or the batch Bezier approach in which the estimate at any point of the trajectory is obtained by best fitting all measurements available, past and future. The EKF estimate at the time of the last measurement is almost identical to the weighted batch least-squares estimate at that same time.

The EKF is initialized with an initial estimate $\hat{\mathbf{x}}_0^T = \{ \hat{\mathbf{r}}_0^T, \hat{\mathbf{v}}_0^T \}$ with associated initial estimation error covariance given by

$$P_0 = \begin{bmatrix} (5 \text{ km})^2 \mathbf{I}_{3 \times 3} & \mathbf{O}_{3 \times 3} \\ \mathbf{O}_{3 \times 3} & (0.01 \text{ km/s})^2 \mathbf{I}_{3 \times 3} \end{bmatrix}$$

The state is propagated forward to the next measurement time using Earth and Moon's central gravities. Together with the state we integrate the state transition matrix $\Phi(t_k, t_{k-1})$ that takes linearized state deviations from the prior measurement time to the current measurement time. This is different from batch least-squares where the state transition matrix was always referring to the initial epoch. In-between measurements the covariance is propagated as

$$P_k = \Phi(t_k, t_{k-1}) P_{k-1}^+ \Phi(t_k, t_{k-1})^T$$

notice the absence of process noise. The measurement update is given by

$$K_k = P_k \tilde{H}_k^T (\tilde{H}_k P_k \tilde{H}_k^T + \Sigma_k)^{-1} \quad (28)$$

$$\hat{\mathbf{x}}_k^+ = \hat{\mathbf{x}}_k + K_k [\tilde{\mathbf{y}}_k - (\mathbf{r}_{mk} - \hat{\mathbf{r}}_k)] \quad (29)$$

$$P_k^+ = P_k - K_k (\tilde{H}_k P_k \tilde{H}_k^T + \Sigma_k) K_k^T \quad (30)$$

where \tilde{H}_k and Σ_k are defined in Eqs. (21) and (26), respectively.

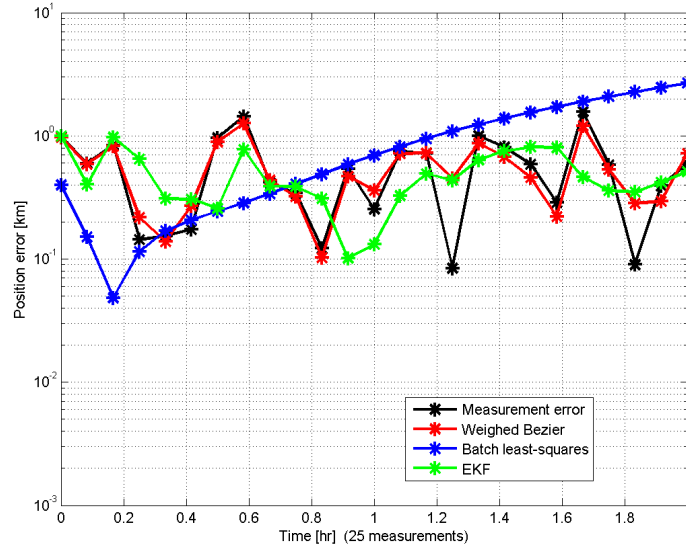


Figure 11. Position estimation error along segment 1.

CONCLUSIONS

REFERENCES

- [1] de Dilectis, F. and Mortari, D. and Zanetti, R. "Trajectory Determination with Unknown Perturbations," *Proceedings of 2013 AAS/AIAA Astrodynamics Specialist Conference*, Hilton Head, SC, August 11-15, 2013.

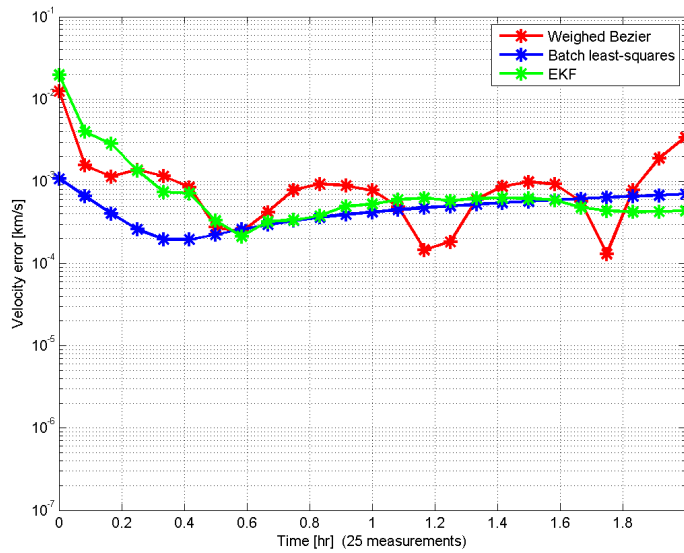


Figure 12. Velocity estimation error along segment 1.

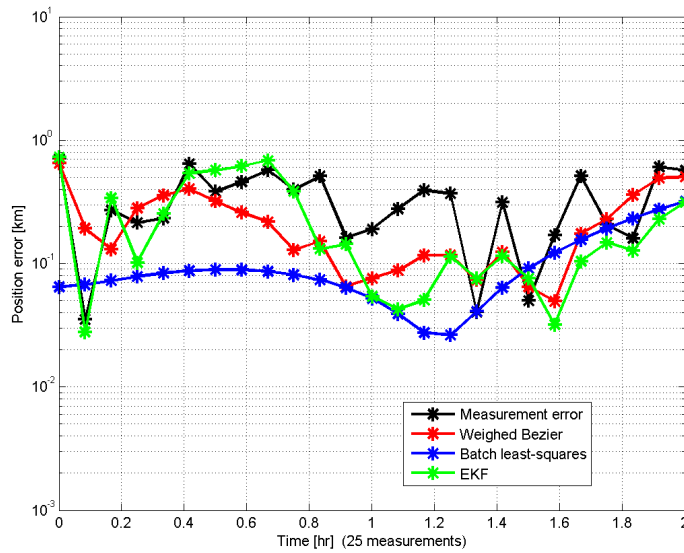


Figure 13. Position estimation error along segment 2.

- [2] Howell, K.C. and Pernicka, H.J. "Initial orbit determination - The pragmatist's point of view," *The Astronomical Journal*, Vol. 90, August 1985, pp. 1541-1547.
- [3] Bellman, Richard and Kagiwada, Harriet and Kalaba, Robert "Orbit Determination as a Multi-Point Boundary-Value Problem and Quasilinearization," *Proceedings of the National Academy of Sciences of the United States of America*, Vol. 48, No. 8, August, 1962.
- [4] Howell, K.C. and Pernicka, H.J. "Numerical determination of Lissajous trajectories in the restricted three-body problem," *Celestial Mechanics*, Vol. 41, No. 1-4, 1987, pp. 107-124.
- [5] Tapley, B.D. "Recent Advances in Dynamical Astronomy," *Astrophysics and Space Science Library*,

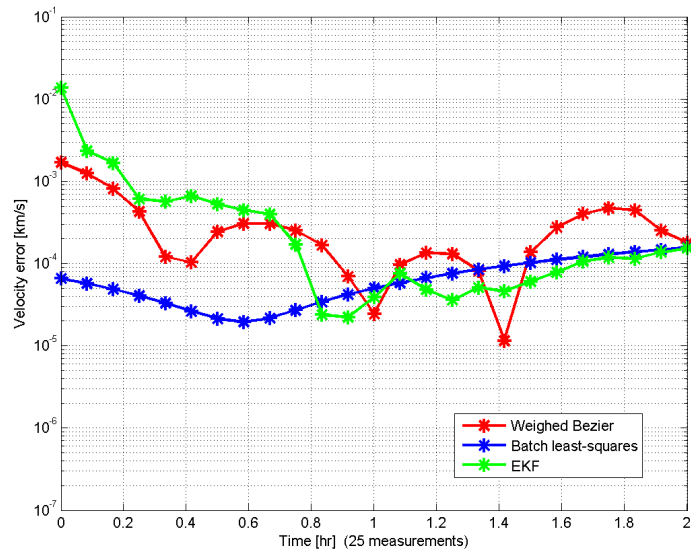


Figure 14. SVelocity estimation error along segment 2.

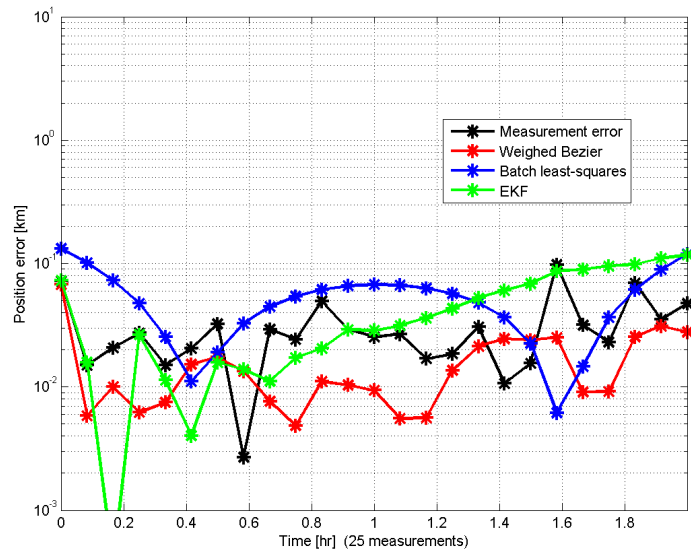


Figure 15. Position estimation error along segment 3.

Vol. 39, 1973, pp. 396-425.

- [6] DeMars, Kyle J. and Jah, Moriba K. "Probabilistic Initial Orbit Determination Using Gaussian Mixture Models," *Journal of Guidance, Control and Dynamics*, Vol. 36, No. 5, September, 2013, pp. 1324-1335.
- [7] Yang, Ying and Yang, XuHai and Li, ZhiGang and Feng, ChuGang "Satellite orbit determination combining C-band ranging and differenced ranges by transfer," *Chinese Science Bulletin*, Vol. 58, No. 19, July, 2013, pp. 2323-2328.
- [8] Li, Wenwen and Li, Min and Shi, Chuang and Zhao, Qile "Jason-2 precise orbit determination using DORIS RINEX phase data," *Geomatics and Information Science of Wuhan University*, Vol. 38, No.

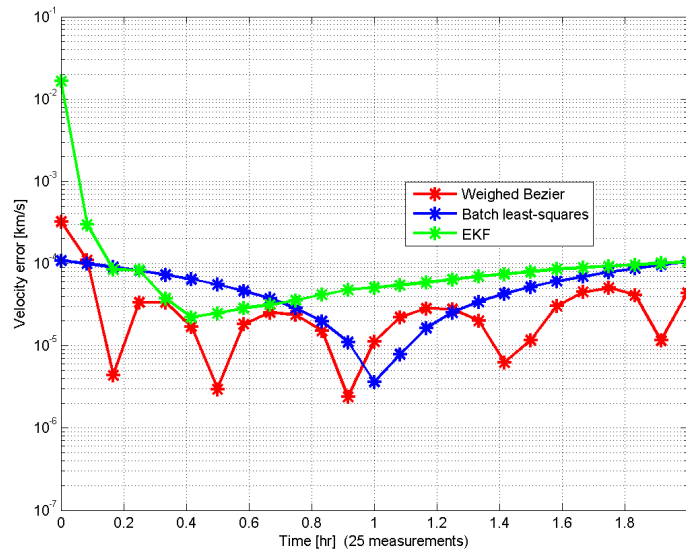


Figure 16. Velocity estimation error along segment 3.

10, October, 2013, pp. 1207-1211.

[9] Zhang,Xiaohong and Li,Pan and Zuo,Xiang “Kinematic precise orbit determination based on ambiguity-fixed PPP,” *Geomatics and Information Science of Wuhan University*, Vol. 39, No. 9, September, 2013, pp. 1009-1013.

[10] Byron D. Tapley et al., *Statistical Orbit Determination*, Elsevier Academic Press, 2004.